ISSN 1726-5479

SENSORS & TRANSDUCERS

vol. 20
Special
4/13

Sensors, Networks, Control Systems and Information Processing

International Frequency Sensor Association Publishing

Sensors & Transducers

International Official Journal of the International Frequency Sensor Association (IFSA) Devoted to Research and Development of Sensors and Transducers

Volume 20, Special Issue, April 2013

Editor-in-Chief
Sergey Y. YURISH

IFSA Publishing: Barcelona • Toronto

Printed in the USA.

Sensors & Transducers

Volume 20, Special Issue, April 2013 **www.sensorsportal.com** **ISSN 2306-8515 e-ISSN 1726-5479**

Sensors & Transducers Journal (ISSN 2306-8515) is a peer review international journal published monthly online by International Frequency Sensor Association (IFSA). Available in both: print and electronic (printable pdf) formats.

Sensors & Transducers Journal

Contents

Volume 20
Special Issue
April 2013

www.sensorsportal.com

ISSN 1726-5479

Research Articles


IARIA
The Fourth International Conference on Sensor Device Technologies and Applications
SENSORDEVICES 2013
25 - 31 August 2013 - Barcelona, Spain
Tracks: Sensor devices - Ultrasonic and Piezosensors - Photonics - Infrared - Gas Sensors - Geosensors - Sensor device technologies - Sensors signal conditioning and interfacing circuits - Medical devices and sensors applications - Sensors domain-oriented devices, technologies, and applications - Sensor-based localization and tracking technologies - Sensors and Transducers for Non-Destructive Testing
Deadline for papers: 30 March 2013
http://www.iaria.org/conferences2013/SENSORDEVICES13.html


IARIA
The Seventh International Conference on Sensor Technologies and Applications
Deadline for papers: 30 March 2013
SENSORCOMM 2013
25 - 31 August 2013 - Barcelona, Spain
Tracks: Architectures, protocols and algorithms of sensor networks - Energy, management and control of sensor networks - Resource allocation, services, QoS and fault tolerance in sensor networks - Performance, simulation and modelling of sensor networks - Security and monitoring of sensor networks - Sensor circuits and sensor devices - Radio issues in wireless sensor networks - Software, applications and programming of sensor networks - Data allocation and information in sensor networks - Deployments and implementations of sensor networks - Under water sensors and systems - Energy optimization in wireless sensor networks
http://www.iaria.org/conferences2013/SENSORCOMM13.html


IARIA
The Sixth International Conference on Advances in Circuits, Electronics and Micro-electronics
CENICS 2013
25 - 31 August 2013 - Barcelona, Spain
Deadline for papers: 30 March 2013
Tracks: Semiconductors and applications - Design, models and languages - Signal processing circuits - Arithmetic computational circuits - Microelectronics - Electronics technologies - Special circuits - Consumer electronics - Application-oriented electronics
http://www.iaria.org/conferences2013/CENICS13.html

Sensors & Transducers, Vol. 20, Special Issue, April 2013, pp. 37-45

Sensors & Transducers

http://www.sensorsportal.com

An Improved Phase-Coherent Algorithm for High Dynamic Doppler Simulation in Navigation Simulator

Qi Wei, Guo Junhai, Liu Guangjun, Luo Haiying, Wang Jing
Beijing Institute of Tracking and Telecommunications Technology, Beijing 100094, China
Tel.: +86-10-66360553
E-mail: robyche@163.com

Received: 1 February 2013 /Accepted: 17 April 2013 /Published: 30 April 2013

Abstract: Research targeting high dynamic Doppler frequency shift (DFS) algorithms in navigation signal simulator has important practical value. An improved Doppler simulation algorithm based on phase-coherent strategy suitable is proposed. Based on Software Radio architecture and the real-time resolving carrier high dynamic moving model, the DFS can be mapped to the phase difference between satellite signal pseudo code and carrier. The dynamic signal modulation can be implemented with the configurable numerically controlled oscillator (NCO). The quantization error and sampling error during simulation can also be eliminated by the synchronization checking algorithm of NCO frequency control word. This work guarantees the signal simulator can run constantly for a long time stably and also has the advantages of high precision and low-complexity. The simulation results from the simulator are compared with synchronous positioning results from the receiver, which demonstrate that not only the output signals of the simulator can accurately reflect the dynamic changes of the carrier, but also the high dynamic simulated signals are consistent with the rules of the real satellite signal's Doppler characteristics. *Copyright © 2013 IFSA.*

Keywords: Satellite navigation, Signal simulator, DFS simulation, High dynamics, Phase-coherent, Configurable NCO.

1. Introduction

Being the critical testing tools in the research area of satellite navigation system, the signal simulator can flexibly simulate satellite transmitting signals in various environment conditions. This device can provide reliable, stable, accurate and operative simulating and testing environments for the development, construction and testing of navigation terminal system [1-3]. Promoted by both upgraded existing navigation systems and construction of new navigation systems, advanced simulation instruments are highly desired to validate the navigation techniques and algorithms. These developing trends raise newer and higher requirements for satellite signal simulation and testing technology.

The research of high dynamic satellite signal simulator includes many complex techniques such as the precise control of pseudo code and carrier frequency, dynamic signal modulation, measurement error simulation, and so on [4-5]. During the test aiming to the high performance receiver, dynamic Doppler simulation is a key technique, which needs to be solved. In the high dynamic environment, the high speed relative movement between the satellite and the receiver will cause continual DFS in the receiving signal [6]. In order to verify and evaluate the processing ability of the receiver to high dynamic signals, the satellite signals transmitted by signal simulator should have real high dynamic Doppler characteristic.

At present, the signal simulation precision in the high dynamic environment is considered as a critical performance measurement of navigation simulators [7]. The GSS8000 simulator from England spirant company implements the high dynamic signal simulation based on the user moving track. In China, universities and research institutions such as Beijing University of Aeronautics and Astronautics, National University of Defense Technology and OlinkStar company, which have always been engaged in the research of navigation signal simulators, have made some achievements in the high dynamic signal simulation during recent years. However, the mature theory of the simulation to dynamic Doppler effects has not been built and there is no detailed algorithm in the related references.

This paper proposes a DFS simulation algorithm based on the phase-coherent mode. By mapping the DFS of satellite signals to the phase difference between satellite signal pseudo code and carrier, the simulator can implement the dynamic signal under the condition of continuous changing Doppler frequency. Based on a close-loop synchronization checking algorithm, the optimized design of signal simulation precision can be implemented with available system resource in the hardware system.

2. High Dynamic Navigation Signal Simulator

The high dynamic navigation simulator can mainly be applied to test the receiver’s capture track performance and carry out the precise evaluation in dynamic environment. The main features of simulator are generating high dynamic signals according to the carrier's actual trajectories, simulating the received satellite signals of receiver with continuous dynamic changes accurately, and reflecting the Doppler frequent shift changes of the relative movement between navigation satellites and carrier [8-9] in real time.

In recent research results, it’s possible to implement the accurate simulation of navigation signal under high dynamic conditions with the programming technique such as Matlab or C language, which is of good flexibility. However, the software signal simulation platform can only be used as theoretical or algorithm analysis tool because of it can’t realize the real time signal generation. This configuration can’t have considerably practical significance for engineering.

In this paper, a hardware/software cooperated architecture is adopted to establish the navigation signal simulator, which is primarily composed of an IF signal processing unit based on software radio (SR) architecture [10], a flexible data simulation and display control system on the computer and complete closed-loop testing interfaces.

Based on the architecture composed of computer (PC), Digital Signal Processor (DSP) and Field Programmable Gate Array (FPGA), the high dynamic navigation simulator primarily includes PC communication module, information processing module, signal processing module and bus information exchange module. The simulator carries out carrier trajectory simulation and ephemeris analysis through PC communication module, and generates signal controlling parameters according to the simulation environment in real time. Being the central components of the simulator, information processing module and signal processing module are respectively implemented in the DSP and FPGA platforms to implement the simulation of updated constellation information, dynamic pseudo code and carrier generation, real-time satellite position calculating, navigation data generation and the baseband and Intermediate Frequency (IF) signal modulation. Simulation data exchanging and buffering are completed in the bus information exchange module. The Radio Frequency (RF) signal of the simulator can be obtained from digital IF signals through the operation of D/A conversion and modulation. The overall architecture of the high dynamic signal simulator is shown in Fig. 1.

As can be seen from Fig. 1, with the flexible simulation calculation in information processing module based on software platform retained, the system architecture can make full use of the advantages of the high-speed signal processing of DSP and FPGA chips, and achieves real-time simulation and output of the high dynamic signal.

3. Algorithm of the Dynamic Doppler Simulation

In satellite navigation system, the relative motion between a moving carrier and a navigating satellite will produce DFS between signals transmitted by the satellite and signals received by the receiver.

$$f_d = f_t - f_r = \pm f_t \bullet v / c, \tag{1}$$

where f_t is the satellite transmitted frequency, f_r is the received signal frequency, v=[v_x , v_y ,v_z]^T is the receiver vector motion velocity related to the satellite, c is the light speed. The Doppler frequency has a positive polarity when the satellites approach close to the receiver.

The Doppler Effect in high dynamic environment results that navigation satellite signal has remarkable frequency dynamic drift property. In the following sections a kind of phase-coherent Doppler simulation algorithm based on a specific carrier moving model is described.

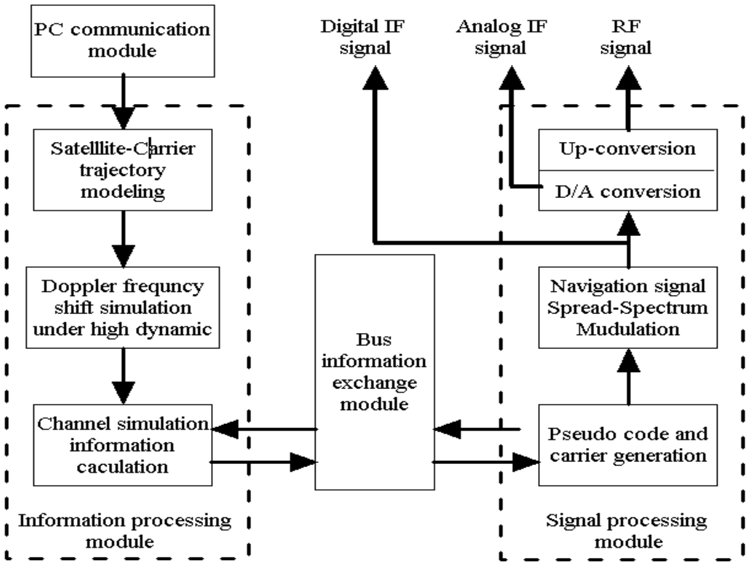

Fig. 1. System architecture of high dynamic signal simulator.

3.1. Dynamic Signal Based on Carrier Trajectory

The motion track model of high dynamic carrier is mainly constructed by its dynamic parameters. Assume that the moving carrier moves with variable speeds relative to the satellite, then its basal moving model can be described as:

$$\begin{cases} \boldsymbol{d}(t_{n+1}) = \boldsymbol{v}(t_n)t_s + \boldsymbol{a}(t_n)t_s^2/2 + \boldsymbol{j}(t_n)t_s^3/6 \\ \boldsymbol{v}(t_{n+1}) = \boldsymbol{v}(t_n) + \boldsymbol{a}(t_n)t_s + \boldsymbol{j}(t_n)t_s^2/2 \\ \boldsymbol{a}(t_{n+1}) = \boldsymbol{a}(t_n) + \boldsymbol{j}(t_n)t_s \end{cases}, \quad (2)$$

where $\boldsymbol{d}$ means the carrier moving displacements, $\boldsymbol{v}$ is the vector velocity, $\boldsymbol{a}$ is the vector accumulation, $\boldsymbol{j}$ is the vector jerk and $t_s = t_{n+1} - t_n$ means sampling time interval.

In the satellite navigation signal simulator, the dynamic information of carrier reflects in the system output signal, which can be expressed as follow [11-12]:

$$\begin{aligned} S_R(t) &= \sum\nolimits_i A_i D_i G_i [f_G(t-\tau_i) + \varphi_{i0}] \\ &\times \cos[2\pi f_R(t-\tau_i) + \phi_{i0}] \end{aligned}, \quad (3)$$

where i means the satellite number, A means the signal amplitude, D means the navigation data, G_i means the pseudo code, f_G and f_R mean the pseudo code and carriers' transmitting frequencies respectively, φ_{j0} and ϕ_{j0} mean the initial phase of satellite pseudo code and carrier respectively.

In Eq.(3), τ_i is the transmission delay of the i^{th} satellite's signal to the receiving antenna RF front-end:

$$\tau_i = R/c + \Delta d + \Delta clk + \Delta ion + \Delta trop, \quad (4)$$

where R means the real distance between the satellite and receiver, Δd means the DFS delay, Δclk means the satellite clock error delay, Δion means the ionospheric delay and $\Delta trop$ means the tropospheric delay [13].

Eq. (4) explains that the propagation delay includes the real distance transmitting time and the delay caused by various errors of transmission environment. According to the carrier motion trajectory proposed in Eq. (2), when only the DFS error model is considered, assuming the vector distance between the receiver and the ith satellite at the initial time to $\boldsymbol{R_i}$, then the system signal receiving delay can be rewritten as follows:

$$\begin{aligned} \tau_i &= R/c + \Delta_d = [|\boldsymbol{R_i}| - |\boldsymbol{v}(t)|t_s]/c \\ &= [|\boldsymbol{R_i}| - (|\boldsymbol{v}| + |\boldsymbol{a}|t_s + |\boldsymbol{j}|t_s^2/2)t_s]/c \end{aligned}, \quad (5)$$

The signal $S_R(t)$ is down-converted by the RF front-end of receiver and the high frequency part is eliminated through a low-pass filter. Set the down-conversion local oscillation frequency is f_o, then the IF signal with nominal frequency f_{RF} can be obtained as follows:

$$\begin{aligned} S_I(t) &= \sum\nolimits_i AD_i\{f_G t - f_G[|\boldsymbol{R_i}| - (|\boldsymbol{v}| + |\boldsymbol{a}|t_s \\ &+ |\boldsymbol{j}|t_s^2/2)t_s]/c + \varphi_{i0}\}\cos\{2\pi f_i t + 2\pi f_R \\ &[(|\boldsymbol{v}| + |\boldsymbol{a}|t_s + |\boldsymbol{j}|t_s^2/2)t_s]/c - 2\pi f_R|\boldsymbol{R_i}|/c + \phi_{i0}\} \end{aligned}, \quad (6)$$

where $f_i = f_R - f_o$, $S_I(t)$ means the satellite IF signal generated by the simulator at the receiving time. The affect to satellite transmitting signal from DFS is obvious in Eq.(6).

3.2. Doppler Effect in Phase-coherent Algorithm

During the digital signal processing, $S_I(t)$ should be sampled as the discrete-time signal. Set the system sampling time interval as T_s, and the signal output at the time of $t_s = nT_s$ is:

$$\begin{aligned} S_I(n) &= \sum_i AD_i\{ f_G t + f_G[|\boldsymbol{v}| + |\boldsymbol{a}| nT_s \\ &+ |\boldsymbol{j}|(nT_s)^2/2] \times nT_s/c - f_G|\boldsymbol{R_i}|/c + \varphi_{i0}\} \\ &\times \cos\{2\pi f_I t_s + 2\pi f_R[|\boldsymbol{v}| + |\boldsymbol{a}| nT_s + \\ &|\boldsymbol{j}|(nT_s)^2/2]nT_s/c - 2\pi f_R|\boldsymbol{R_i}|/c + \phi_{i0}\} \end{aligned}, \quad (7)$$

At the time of (n+1)T_s, the output sampling signal is:

$$\begin{aligned} S_I(n+1) &= \sum_i AD_i\{ f_G t - f_G|\boldsymbol{R_i}|/c + \varphi_{i0} + \\ &f_G[|\boldsymbol{v}| + |\boldsymbol{a}|(n+1)T_s + |\boldsymbol{j}|(n+1)^2T_s^2/2](n+1)T_s/c\} \\ &\times\cos\{ 2\pi f_I t + 2\pi f_R[|\boldsymbol{v}| + |\boldsymbol{a}|(n+1)T_s + \\ &|\boldsymbol{j}|(n+1)^2T_s^2/2](n+1)T_s/c - 2\pi f_R|\boldsymbol{R_i}|/c + \phi_{i0}\} \end{aligned}, \quad (8)$$

According to Eq.(7)-(8), the phase increment of the pseudo code and carrier from time nT_s to time $(n+1)T_s$ can be respectively obtained as:

$$\begin{aligned} \Delta\varphi_G^i = {} & f_G[|\boldsymbol{v}| + |\boldsymbol{a}|(2n+1)T_s \\ &+ |\boldsymbol{j}|(3n^2+3n+1)T_s^2)/2]T_s/c \end{aligned}, \quad (9)$$

$$\begin{aligned} \Delta\phi_C^i = {} & 2\pi f_R[|\boldsymbol{v}| + |\boldsymbol{a}|(2n+1)T_s \\ &+ |\boldsymbol{j}|(3n^2+3n+1)T_s^2)/2]T_s/c \end{aligned}, \quad (10)$$

From Eq.(9)-(10), the phase change of pseudo code and carrier in each sampling time can be calculated, and the phase of pseudo code and carrier in next sampling period can be obtained [14]. From the deduction above, it can be seen that the main embodiment for the phase-coherent DFS simulation lies in the phase difference of the pseudo code and the carrier between two adjacent sampling times.

3.3. Dynamic Phase Difference Calculation

To simplify the algorithm in the navigation signal simulator, the DFS simulation can be implemented by establishing the relationship between the displacement differences of motion target and transmitted signal phase differences in sampling time intervals. In the process of high dynamic simulation, parameters such as distance and velocity can be calculated by the carrier motion model. If system sampling rate is high enough, the displacement and velocity in the consecutive sampling moment would satisfy the following equation:

$$\begin{aligned} \Delta\boldsymbol{d}_i &= \int_{nT_s}^{(n+1)T_s} \boldsymbol{v}(t)dt \\ &= \int_{nT_s}^{(n+1)T_s} (\boldsymbol{v} + \boldsymbol{a}t_s + \boldsymbol{j}t_s^2/2)dt_s \end{aligned}, \quad (11)$$

Combining Eq.(7), Eq.(8) and Eq.(11), it can be obtained as:

$$\begin{aligned} \Delta\varphi_G^i &= S_I(n+1) - S_I(n) = f_G[|\boldsymbol{v}| + \\ &|\boldsymbol{a}|(2n+1)T_s + |\boldsymbol{j}|(3n^2+3n+1)T_s^2)/2]T_s/c \\ &= \left[\int_{nT_s}^{(n+1)T_s} (|\boldsymbol{v}| + |\boldsymbol{a}|t_s + |\boldsymbol{j}|t_s^2/2)dt_s\right] f_G/c \\ &= f_G|\Delta\boldsymbol{d}_i|/c = |\Delta\boldsymbol{d}_i|/\lambda_G \end{aligned}, \quad (12)$$

Based on Eq. (12), the dynamic pseudo code phase difference can be mapped to the quotient between the displacement distance and the pseudo code wavelength during the moving time. With the same method, the phase difference of the carrier can obtained as:

$$\Delta\phi_C^i = |\Delta\boldsymbol{d}_i|/\lambda_C, \quad (13)$$

In summary, the transformation between the pseudo code and the carrier's DFS can be denoted as follows:

$$F_{dG}^i = |\boldsymbol{v}(t)| f_G/c = \Delta\varphi_G^i/T_s = |\Delta\boldsymbol{d}_i|/\lambda_G T_s, \quad (14)$$

$$F_{dC}^i = |\boldsymbol{v}(t)| f_R/c = \Delta\phi_C^i/2\pi T_s = |\Delta\boldsymbol{d}_i|/2\pi\lambda_C T_s, \quad (15)$$

where F^i_{dG} and F^i_{dC} are the Doppler frequencies of the pseudo code and carrier respectively, $\Delta\varphi^i_G$ and $\Delta\phi^i_C$ are the phase differences of the pseudo code and carrier of the ith satellite in the sampling time interval respectively.

Based on this conclusion, displacement difference of each sampling moment can be calculated by the relationship between the velocity variety and moving distance. The simulation of dynamic DFS can be implemented through the calculation of phase differences, which are the ratios of displacement difference at each sampling time and the wavelength. This processing method simplifies the complexity of the Doppler simulation algorithm significantly.

4. Implement of Dynamic Signal Simulation

4.1. Signal Modulation by Configurable NCO

In order to implement the modulation of high dynamic pseudo code and carrier quickly and precisely, we propose a compatible and configurable NCO design scheme, which generates the pseudo code and the carrier frequency including Doppler characteristic by the real time accumulation of NCO control word.Configurable NCO consists of pseudo code generator module and carrier generator module. Every module carries out the NCO accumulation through the initial phase control word and the dynamic frequency control word. Assuming $\boldsymbol{R_{i0}}$ as the vector distance between the ith satellite and the receiver at the starting time of the simulation. The initial phase of the pseudo code and the carrier can be obtained as follows:

$$\varphi_{i0} = |\boldsymbol{R_{i0}}| / c\lambda_G = f_G |\boldsymbol{R_{i0}}| / c, \quad (16)$$

$$\phi_{i0} = 2\pi |\boldsymbol{R}_{i0}| / c\lambda_C = 2\pi f_C |\boldsymbol{R}_{i0}| / c, \quad (17)$$

According to the principle of NCO accumulation, initial phase control words correspond to the decimal fraction part, and are considered as the phase offset of NCO frequency accumulator:

$$\Phi^i_{G0} = (\varphi_i - M^i_G)2^N, \quad (18)$$

$$\Phi^i_{C0} = (\phi_i - 2\pi M^i_C)2^N, \quad (19)$$

where $M^i_{\boldsymbol{G}}$ and $M^i_{\boldsymbol{C}}$ are the whole chips counter and the integer carrier periods corresponding to the initial transmission delay of the ith satellite transmitted signal respectively, N means the binary quantization bit width of the control word.

By calculating the relative positions of the satellites and the carrier based on the carrier motion model and satellite ephemeris, the displacement difference $\Delta\boldsymbol{d_i}$ between two adjacent calculation periods can be obtained. Following the conclusion of Eq.(14)-(15), we can obtain the pseudo-code and the carrier's frequency which have Doppler dynamic characteristics, and then quantize them to the binary form , which are used as control words of the NCO frequency accumulator.

$$\begin{aligned} W^i_G(n) &= (f_G + F^i_{dG})2^N / f_s \\ &= f_G(1 + |\Delta\boldsymbol{d}_i| / cT_s)2^N / f_s \end{aligned}, \quad (20)$$

$$\begin{aligned} W^i_C(n) &= (f_R + F^i_{dC})2^N / f_s \\ &= f_R(1 + |\Delta\boldsymbol{d}_i| / 2\pi cT_s)2^N / f_s \end{aligned}, \quad (21)$$

where f_s means the system sampling frequency. Configurable NCO frequency generator is implemented based on the principle of Direct Digital Frequency Synthesis (DDS) technology [15].

The NCO generates a linear frequency modulation signal. Step time logic unit controls the parameter update rate according to the input time step control word. Frequency step variable control word represents the frequency changing information and makes that the dynamic information such as velocity and acceleration are reflected in the generated frequency.

In pseudo code generator, the initial code phase control word is considered as the initial value accumulator. The code frequency control word $W_{\boldsymbol{G}}(n)$ is considered as the accumulation input, and is accumulated in the code NCO logic at each sampling time. When the accumulated value is $>=2^N$ in the register, the code phase accumulator will overflow, indicating that a whole pseudo code chip period has been passed through. The overflow signal can be considered as the drive clock of the pseudo code generator to implement the generation of high dynamic pseudo code [16].

The NCO accumulation logic of carrier generator is basically identical with that in pseudo code NCO. The carrier NCO is accumulated by configuring the carrier initial phase control word and frequency control word. In each sampling period, the accumulation result is considered as the carrier phase information. According to the phase value, the sine-cosine wave amplitude digital quantization signal can be obtained by looking up the phase-amplitude table [16,17]. The dynamic signal modulation structure based on configurable NCO is elaborated in Fig. 2.

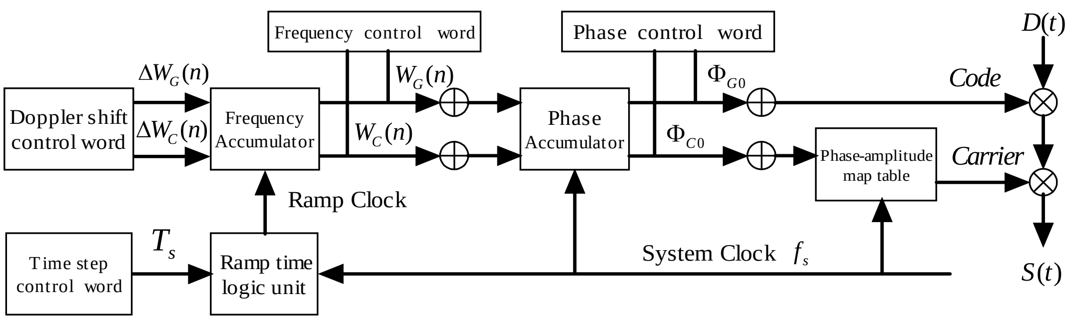

Fig. 2. Architecture of step-type configurable NCO.

In the simulation test platform based on the SR architecture, with respect to the requirement of simulation precision and real-time processing, the period of data calculation T_s in the signal simulation algorithm should be set reasonably according to the computing ability of the FPGA and DSP chip. The pseudo-range simulation precision based on the configurable NCO's signal simulation algorithm can be described as:

$$\Delta P = c/(2^N \cdot f_G), \quad (22)$$

The simulation resolution of DFS based on the signal dynamic characteristic can be described as:

$$\delta \boldsymbol{D} = (f_G \text{g} \boldsymbol{M}) \times T_s / c, \quad \boldsymbol{M} = [v, a, j]^T, \quad (23)$$

Take the pseudo code of 10.23 MHz for example, the NCO quantization bits N=36, the period of data calculation T_s is 1ms. From the Eq. (22)-(23), when the dynamic velocity is 20000 m/s and the acceleration is 1000 m/s^2, the simulation precision of signal pseudo code based on the configurable NCO architecture is about 4.2×10^{-9} m, and the corresponding Doppler frequency resolution of velocity and acceleration is 0.68 Hz and 0.034 Hz/s respectively.

From the analysis above, T_s is important to the simulation performance of high dynamic signal. The configurable NCO, as shown in Fig. 2, can adjust the period of data calculation T_s with the time step control word, configure the quantization bits N by changing frequency control word, phase control word and Doppler shift control word, and obtain optimal signal simulation precision and high dynamic Doppler resolution with high real time of the system guaranteed.

4.2. Emendation of Frequency Control Word

In the design of the configurable NCO frequency generator, the quantization errors and sampling errors are produced during the frequency control word accumulation. These errors will be accumulated with time. The simulation precision of signal pseudo-rage will be affected by the random errors when simulator performs the high dynamic signal simulation. In order to eliminate the effect on the signal simulation precision caused by the errors, the closed-loop frequency control word emendation in signal processing module and information processing module should be carried out.

In each interruption period, the signal processing module transfer the accumulated pseudo code and carrier phase values back to the information processing module. By comparing the pseudo code and carrier phase theory values transferred back with that calculated in the information processing module at the same time, the errors of frequency accumulation within this calculation period can be obtained, and the emendation value of the frequency control word can be computed through the system sampling clock f_s.

Take the pseudo code for example, assuming $P_s(n)$ and $P_t(n)$ are the code NCO accumulation value and real time calculated phase theory value in the nth period respectively, then the emendation value of pseudo code frequency control word in the ($n+1$)th period is:

$$\Delta W_G(n) = [P_t(n) - P_r(n)]/T_s f_s, \quad (24)$$

As a correction value, $\Delta W_G(n)$ is added to $W_G(n)$ in Eq. (20) to obtain the updated frequency control words of NCO frequency generator in the next period so as to implement the closed-loop emendation. The verification in the simulator is carried out by testing the simulation precision in static environment. Fig. 3 and Fig. 4 show the pseudo-range output values of simulator with or without the emendation algorithm respectively.

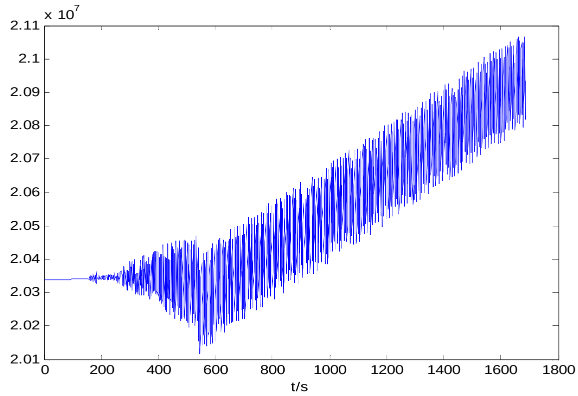

Fig. 3. Pseudo-range simulation data without the emendation algorithm.

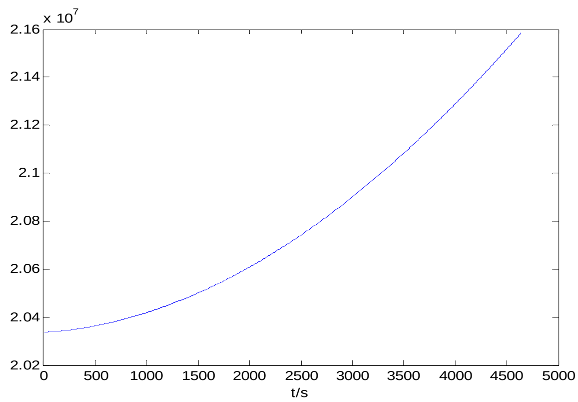

Fig. 4. Pseudo-range simulation data with the emendation algorithm.

By comparing the testing results in Fig. 3 and Fig. 4, it can be obvious seen that the phase error of pseudo-range is reduced from 10^{-2} m to 10^{-5} m, the simulation data with NCO closed-loop emendation are smoother and no jitter occurs. This algorithm can effectively reduce the pseudo-range simulation error and consequently improve the signal accuracy of the simulator.

Based on the mathematical module above, the Algorithmic State Machine (ASM) chart of the simulator system is described in Fig. 5.

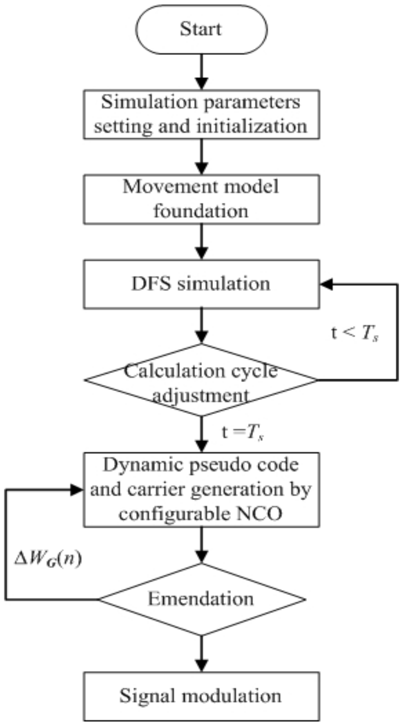

Fig. 5. ASM-chart of dynamic signal simulation algorithm.

In the simulator system, the Doppler information is computed with an interval of T_s in the information processing module in real time, and the quantization frequency control words generated in each interruption moment are sent to the signal processing module to update the configurable NCO frequency generator. Based on the ASM-chart shown in Fig. 5, the setting of simulation parameters is implemented in PC platform, the DFS simulation is implemented in DSP platform, the dynamic pseudo code and carrier generation and emendation are implemented in FPGA platform.

5. Application and Analysis of Test Results

The algorithm proposed can be applied to the DFS simulation of variable accelerated motion, circular motion and curve motion. The NCO control words calculated by these motion models include the dynamic information for various trajectories. The modulated signal is provided with the Doppler characteristic under dynamic environment.

V4SX55 FPGA from Xilinx and C6416 DSP from TI are selected as the main chips for the hardware platform of signal simulator. Take BDS B3 signal for example, the pseudo code frequency is 10.23 MHz and the RF carrier frequency is 1268.52 MHz, and T_s is 20 ms. When the initial velocity is 0 m/s, the acceleration is 200 m/s^2 and the jerk is 20 m/s^3, the Doppler frequency of simulator transmitted signal is compared with the dynamic frequency computed by the navigation receiver. the fitted curve and error analysis of the simulated dynamic signal frequency and the real tracking test results are shown in Fig. 6-Fig. 9.

Through the comparison of the results shown in Fig. 6 and Fig. 8, in the high dynamic environment, DFS variation trends of the pseudo code and carrier in the satellite's transmitted signal can be seen. At the time about 10 s, DFS of pseudo code with an initial frequency of 10.23 MHz is about 83 Hz and DFS of carrier with an initial frequency of 1.2 GHz is about 1.35 kHz. The statistical data demonstrate that dynamic characteristics of transmitted signal in the simulator basically meet the theoretical calculation results.

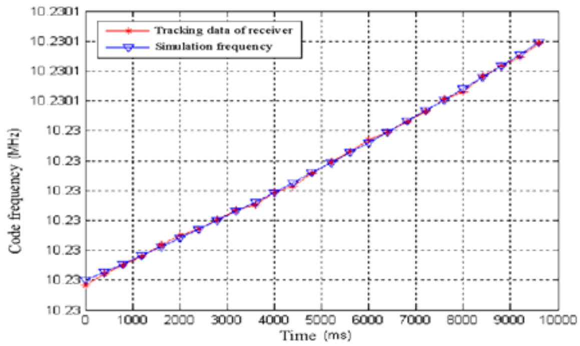

Fig. 6. Curve of the simulated dynamic pseudo code frequency and actual tracking results.

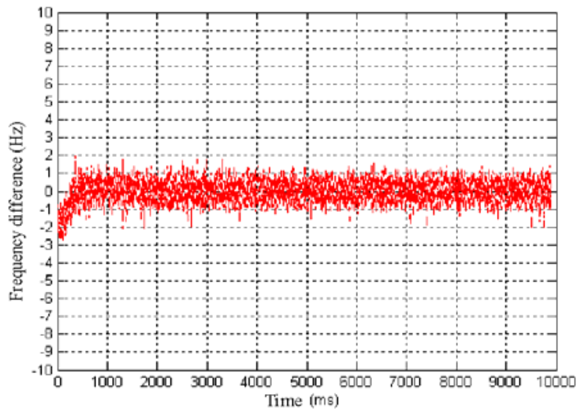

Fig. 7. Difference between the simulated dynamic pseudo code frequency and actual tracking results.

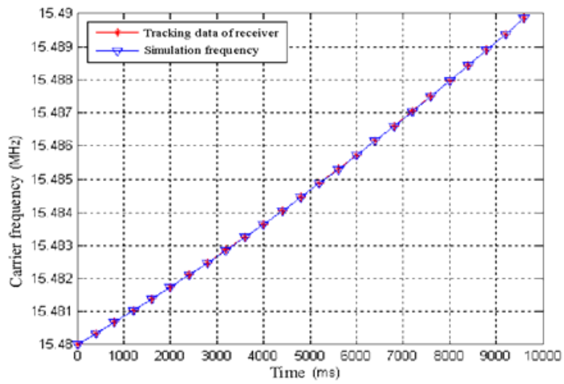

Fig. 8. Curve of the simulated dynamic carrier frequency and actual tracking results.

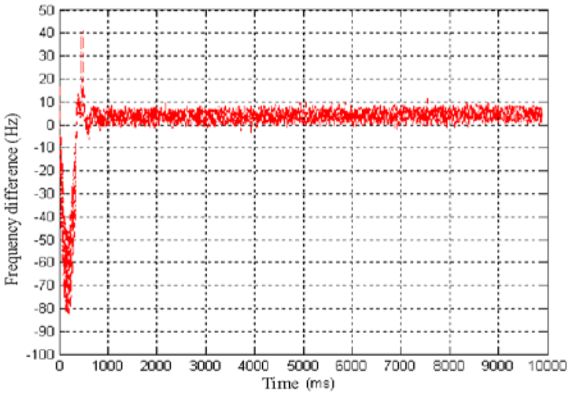

Fig. 9. Difference between the simulated dynamic carrier frequency and actual tracking results.

According to the results of frequency difference shown in Fig. 7 and Fig. 9, frequency jitter of the pseudo code and carrier are within 2Hz and 10Hz separately for the reason that the NCO generators with configurable frequency control words are amended in closed-loop manners during the simulation, which ensures a long time phase-coherent frequency Doppler simulation. The frequency jitter in the initial time of Fig. 8 occurs during the carrier frequency of the receiver tracking loop converges firstly, which is not attributed signal simulation error.

To verify its feasibility and effectiveness, the proposed baseband signal generator based on phase-coherent DFS simulation algorithm is implemented and tested using C code of BDS B3. The resource cost and the simulation precision of pseudo-range are compared with the traditional DFS simulation case. Related parameters in implementation are listed in Table 1.

Table 1. Testing results of main simulation parameters.

	Traditional	Phase-Coherent
Code frequency (MHz)	10.23	10.23
Quantization width (bit)	36	20
Calculation T_s (ms)	4	8
FPGA resource cost (slices)	3937	4009
Pseudo-range precision (m)	6.32×10^{-3}	5.15×10^{-3}

As shown above, the quantization width and calculation *Ts* of phase-coherent structure is only 1/2 of the traditional structure to achieve the same resource consumption and precision level.

Validation and authentication of the output signal from simulator are carried out through the commercial receiver. by comparing the position results with the actual position coordinates of the same time in the carrier's trajectories. Fig. 10 shows the testing results of a group of high dynamic trajectories with carrier orbiting the Earth, which last for 3.5 hours.

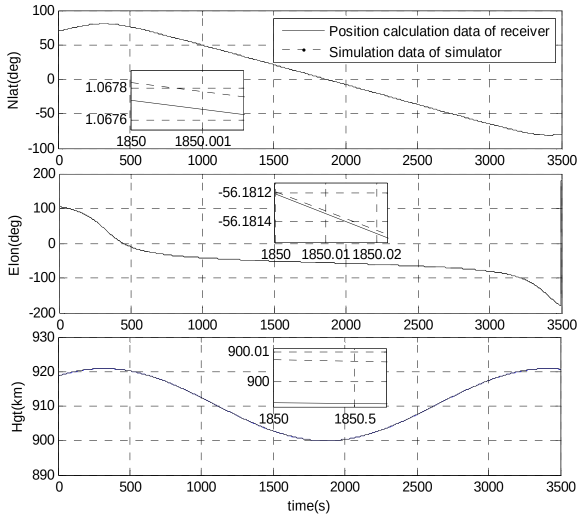

Fig. 10. Location curves of simulated data and the synchronous position result from receiver.

The testing results illustrate that in a long simulation period, position curve output by the receiver is relatively smooth, and its trends are consistent with the original trajectory from the simulator as a whole. This indicates that the simulation data is overall stable, and shows no obvious error or jitter in high dynamic environment. The system can carry out the real-time signal simulation with the data calculation period *Ts* in the rang of 2 ms-50 ms by adjusting the quantization bits of the configurable NCO's control words, in this way , the simulation precision of pseudo range is higher than 0.01 m, and the dynamic Doppler resolution based on L band RF signal is higher than 10 Hz.

6. Conclusions

A Doppler simulation algorithm for the high dynamic signal simulator in the satellite navigation system is proposed. Phase-coherent technique and configurable NCO design are researched to improve the simulation of pseudo code and carrier dynamic frequency shift. The calculation for DFS based on carrier motion models, which optimizes the resource consumption of computation, is discussed in detail. To ensure the signal precision in a long time simulation period, a closed-loop emendation is carried out to correct the NCO frequency control word.

This algorithm is quite simple, comprehensive, robust, and easy to calculate, analyze and simulate the DFS of navigation signals which are used to test the receiver in high dynamics. The architecture based on the configurable NCO satisfies the requirement of system design performance, and is convenient to be upgraded.

The algorithm has already been implemented in a developed Global Navigation Satellite System (GNSS) platform, and has achieved ideal effect of actual tests. All the indexes of the simulator have met the requirements of the project. With higher flexibility and lower complexity of implementation, the algorithm has greater research significance and application value to the navigation satellites signal simulation in high dynamic environment.

Acknowledgements

This work is funded by National High Technology Research and Development Program of China (2009AA12Z313) and National Science Foundation of China (60872062).

References

[1]. Aloi D. N., Alsliety M., Akos D. M., A methodology for the evaluation of a GPS Receiver Performance in telematics applications, *IEEE Transactions on Instrumentation and Measurement*, Vol. 56, Issue 3, 2007, pp. 11-24.

[2]. Lee D. U., Luk W., Villasenor J. D., A Gaussian noise generator for hardware-based simulations, *IEEE Transactions on Computers*, Vol. 53, Issue 12, 2004, pp. 1523-1534.

[3]. Brown A., Gerein N., Modeling and simulation of GPS using software signal generation and digital signal reconstruction, in *Proceedings of the ION National Technical Meeting*, 2000, pp. 646-652.

[4]. Lin Zhao, Jicheng Ding, Shu Yu, All-Digital GPS signal simulating and processing techniques for high dynamic movement, in *Proceedings of the International Workshop on Modelling, Simulation and Optimization*, 2008, pp. 428-432.

[5]. Lie-Chung Shen, Jyh-Ching Juang, Ching-Lang Tsai, Monitoring water levels and currents using reflected GPS carrier Doppler measurements and coordinate rotation model, *IEEE Transactions on Instrumentation and Measurement*, Vol. 59, Issue 1, 2010, pp. 153-163.

[6]. Sun Guoliang, Shen Shituan, Ding Ziming, An integration method for passive RDSS and DNS, *Acta Aeronautica et Astronautica Sinica*, Vol. 27, Issue 4, 2006, pp. 682-686. [in Chinese]

[7]. Lazar S., Bottjer M., A GPS modernization simulator, in *Proceedings of the ION 11th Annual Meeting*, Nashville: The Institute of Navigation, 1998, pp. 1887-1895.

[8]. Tae-Yun Koo, Sung-Ho Ji, Chul-Ho Bae, et al., Development of the GPS simulator for driving simulators, *SICE-ICASE*, in *Proceedings of the International Joint Conference*, 2006, pp. 2133-2137.

[9]. Lazar S., Bottjer M., A GPS modernization simulator, in *Proceedings of the ION 11th Annual Meeting.* Nashville: The Institute of Navigation, 1998, pp. 1887-1895.

[10]. Mitola J., The software radio architecture, *Communications Magazine, IEEE*, Vol. 33, Issue 5, 1995, pp. 26-38.

[11]. Lashley M., Bevly D. M., Hung J. Y., Performance analysis of vector tracking algorithms for weak GPS signals in high dynamics, *IEEE Journal of Selected Topics in Signal Processing*, Vol. 4, Issue 3, 2009, pp. 661-673.

[12]. Kaplan E. D., Understanding GPS Principles and Applications, *Publishing House of Electronics Industry*, 2002.

[13]. Zhao Jun-Xiang, Chang Qing, Zhang Qi-Shan, Zhang Jun, Research of ionospheric time-delay error simulation in high dynamic GPS signal simulator, *Chinese Journal of Aeronautics*, Vol. 16, Issue 3, 2003, pp. 169-176.

[14]. Shan Yuehui, An Wei, Sun Zhongkang, Research on passive locating method using phase rate of change with variant posture of the observer, *Chinese Journal of Aeronautics*, Vol. 15, Issue 3, 2002, pp. 169-170.

[15]. J. Tierney, C. M. Rader, B. Gold, A digital frequency synthesizer, *IEEE Transactions on Audio Eletroacoust*, AU-19, 1971, pp. 48-57.

[16]. Bellaouar A., Low-power direct digital frequency synthesis for wireless communications, *IEEE Journal of Solid State Circuits*, Vol. 35, Issue 3, 2000, pp. 385-390.

[17]. White S. A., Applications of distributed arithmetic to digital signal processing, *IEEE ASSP Magazine*, Vol. 6, Issue 3, 1989, pp. 4-19.

___

Aims and Scope

Sensors & Transducers is a peer reviewed international, interdisciplinary journal that provides an advanced forum for the science and technology of physical, chemical sensors and biosensors. It publishes original research articles, timely state-of-the-art reviews and application specific articles with the following devices areas:

- Physical, chemical and biosensors;
- Digital, frequency, period, duty-cycle, time interval, PWM, pulse number output sensors and transducers;
- Theory, principles, effects, design, standardization and modeling;
- Smart sensors and systems;
- Sensor instrumentation;
- Virtual instruments;
- Sensors interfaces, buses and networks;
- Signal processing and interfacing;
- Frequency (period, duty-cycle)-to-code converters, ADC;
- Technologies and materials;
- Nanosensors;
- Microsystems;
- Applications.

Further information on this journal is available from the Publisher's web site:
http://www.sensorsportal.com/HTML/DIGEST/Submission.htm

Subscriptions

An annual subscription includes 12 regular issues and some special issues. Annual subscription rates for 2013 are the following:

Electronic version (in printable pdf format): 400.00 EUR
Printed with b/w illustrations: 640.00 EUR
Printed full color version: 760.00 EUR

40 % discount is available for IFSA Members.

Prices include shipping costs by mail. Further information about subscription is available through IFSA Publishing's web site: http://www.sensorsportal.com/HTML/DIGEST/Journal_Subscription.htm

Advertising Information

If you are interested in advertising or other commercial opportunities please e-mail sales@sensorsportal.com and your enquiry will be passed to the correct person who will respond to you within 24 hours. Please download also our Media Planner 2013: http://www.sensorsportal.com/DOWNLOADS/Media_Planner_2013.pdf

Books for Review

Publications should be sent to the IFSA Publishing Office: Ronda de Ramon Otero Pedrayo, 42C, 1-5, 08860, Castelldefels, Barcelona, Spain.

Abstracting Services

This journal is cited, indexed and abstracted by Chemical Abstracts, EBSCO Publishing, IndexCopernicus Journals Master List, ProQuest Science Journals, CAS Source Index (CASSI), Ulrich's Periodicals Directory, Scirus, Google Scholar, etc. Since 2011 *Sensors & Transducers* journal is covered and indexed by EI Compendex index (including a Scopus, Embase, Engineering Village and Reaxys) in *Elsevier* products.

Instructions for Authors

Please visit the journal web page http://www.sensorsportal.com/HTML/DIGEST/Submission.htm Authors must follow the instructions very carefully when submitting their manuscripts. Manuscript must be send electronically in both: MS Word 2003 for Windows (doc) and Acrobat (pdf) formats by e-mail: editor@sensorsportal.com